CONCRETE LIBRARY OF JSCE NO. 12. MARCH 1989

A STUDY ON MECHANISM OF TORSIONAL RESISANCE OF REINFORCED CONCRETE MEMBERS

(Reprint from Transaction of JSCE, No.190/V-8, 1988)

Shigeyoshi
NAGATAKI

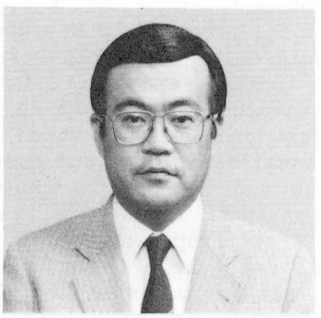

Takahisa
OKAMOTO

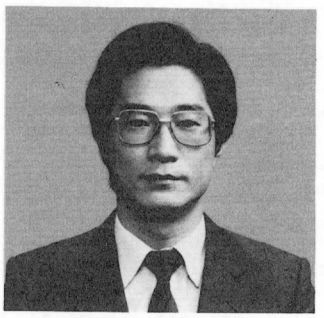

Seung-Han
LEE

SYNOPSIS

An analytical model for predicting the load-deformation responses of reinforced concrete elements subjected to pure torsion is proposed. Compressive stress-strain and tensile stress-strain curves of concrete struts between diagonal cracks are considered in equilibrium in this model.Experiments are then conducted to verify the validity of this model. The experimental and analytical values are found to be in good agreement and the proposed model is thus capable of predicting not only the strengths but also the angles of twist,the steel strains, and the concrete strains throughout the loading history. Concrete cover and reinforcement ratio are also found to have significant effect on the change of shear flow.

S.Nagataki is a professor of civil engineering at Tokyo Institute of Technology, Tokyo, Japan. He received his Doctor of Engineering Degree from Tokyo University in 1966. His research interestes cover physical and chemical properties of concrete, durability of concrete, properties of high strength concrete, effective utilization of additives and torsional behaviors of reinforced concrete members. He was awarded two JSCE prizes (Yoshida Prize) for a study of expansive cement and concrete in 1972 and a study of torsional resistance of reinforced concrete members in 1987, a Cement Association prize for a study of flyash concrete in 1984 and received a ACI fellow in 1986. Dr. Nagataki is a member of ACI, ASCE, RILEM, JSCE, JCI and JSMS.

T.Okamoto is a reseach associate of civil engineering at Tokyo Institute of Technology, Tokyo, Japan. He received his Doctor of Engineering Degree from Tokyo Institute of Technology in 1987. His research interests include shearing and torsional behaviors of reinforced concrete members and mechanical behaviors of repaired concrete structure. He was awarded a JSCE prize (Yoshida Prize) for a study of torsional behaviors of reinforced concrete members in 1987 and a Cement Association prize for a study of the strength of reinforced concrete beams subjected to shear and torsion in 1982. He is a member of ACI, JSCE and JCI.

S.H. Lee is a assistant professor of civil engineering at Keimyung University, Taegu, Korea. He received his Doctor of Engineering Degree from Tokyo Institute of Technology in 1988. His research interests include the mechanical properties of reinforced and prestressed concrete members subjected to pure torsion. He is a member of JSCE, KSCE and JCI.

1. INTRODUCTION

The three-dimensional truss model proposed by Rausch[1] in 1929 and the diagonal flexure model proposed by Lessig[2] in 1959 typical failure models of reinforced concrete members subjected to torsion, and theoretical and experimental studies based on these models have been made extensively up to this time. For example, the strength computation formula proposed by Rausch was found in later studies to overestimate ultimate torsional resistance and numerous corrections have been made. The research by Collins and Mitchell[3] applying the Compression Field Theory based on the three-dimensional truss model maintained that the concrete cover outside the center line of stirrups would be spalled and not contribute to strength, and a correction was made taking shear flow to be inside the center line of stirrups. Further, there is the study by Hsu and Mo[4] that concrete struts between diagonal cracks are in a biaxial compressive-tensile stress state, there being a difference from a uniaxial compression state. These corrections all strictly concern behaviors of reinforced concrete members in the vicinity of ultimate torsional resistance, and although there is an unclear part remaining with regard to handling of cover concrete, so far as ultimate strength is concerned, a stage where they can be used to and an extent in design has been reached.

At present, the world-wide trend is for transition to limit state design, and in the "Design Volume" of the Standard Specifications of the Japan Society of Civil Engineers revised in 1986, it was stipulated that safety be verified concerning serviceability limit state, ultimate limit state, and fatigue limit state. As a result, it became possible to adequately deal with crack resistance and ultimate strength using the concept in current specifications, but there are many theoretically unresolved parts in examination of the serviceability limit state concerning crack width and deformation-displacement, crack width being dealt with by emprical formula while there is nothing on deformation-displacement. Consequently, it is absolutely necessary for rational designing of this type of member to derive theoretical formulae making possible accurate estimates of crack occurrence, behaviors of reinforcement and concrete after crack occurrence, and, deformation behavior.

With this kind of background, there have been many studies made using conventional three-dimensional truss models and diagonal flexure models to analytically examine deformation behaviors at any loading stage, in particular, immediately after occurrence of cracking. Representative ones among such studies are those of Collins and Mitchell[3] and Hsu and Mo[4] using three-dimensional truss models, and of Rangan and Staley[5] and Ewida and McMullen[6] using diagonal flexure models, but these models which consider the ultimate torsional behavior are not capable of expressing the torsional behaviors at arbitrary loading states, especially, just after cracking has occurred. The reason for this is that both models are predicated on a state where diagonal cracks have been completely developed, and tension stiffening of concrete after occurrence of cracking has been ignored.

Therefore, in the present study, tension stiffening of concrete and the influence of cover concrete on torsional behaviors of reinforced concrete

members were focused on.That is, a model introducing tension stiffening of concrete to continuously grasp the torsional behaviors before and after crack occurrence was set out, reinforced concrete members subjected to torsion were extracted, an equilibrium equation considering not only the allocation of compressive force to concrete struts between diagonal cracks, but also tension stiffening of concrete, and a constitutive equation based on the adaptation condition equation of strain were derived, and a new formula for evaluating torsional behavior at any loading condition was obtained. Further, specimens varying thicknesses of concrete cover and reinforcement ratios were made and loading tests were performed with the objective of finding the influences of cover concrete and reinforcement ratio on the torsional resistance behavior of this type of member. The influence of cover on torsional behavior was evaluated, along with which quantitative assessments of analytical results were made based on the results of these experiments, in aiming to explain the torsional resistance of reinforced concrete members (hereafter referred to as "RC members").

2. ANALYTICAL STUDY

2.1 Assumptions in Analysis

a) Compressive Stress-Strain curve of concrete

The compressive stress-strain curve of concrete in the CEB-FIP Model Code which is a representative example of uniaxial compression and that of Vecchio and Collins[10] of a biaxial state subject to compression and tension are shown in Fig. 1.

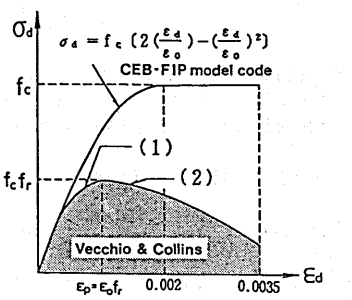

Fig.1 Compressive Stress-Strain Curve of Concrete

In this analysis of RC members subjected to torsion, since concrete between diagonal cracks is under compression-tension of a biaxial state due to tensile force of reinforcement cutting across it, the curve of Vecchio and Collins which considers the stress-strain curve of concrete to be greatly lowered compared with compressive strength of the concrete in a uniaxial state, as shown in Fig. 1, was used. Strains were considered to be distributed in fan shape, while cracking angles at the surfaces and interiors of members were assumed to be identical.

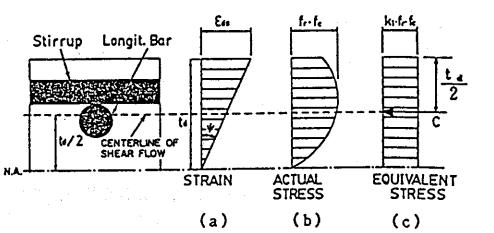

Fig.2 Strain and Stress Distribution in Pass Width of Shear Flow

Case of $\varepsilon_{ds} \leqq \varepsilon_p$

$$\sigma_d = f_r \cdot f_c \left[2\left(\frac{\varepsilon_d}{\varepsilon_p}\right) - \left(\frac{\varepsilon_d}{\varepsilon_p}\right)^2 \right] \qquad \text{------(1)}$$

Case of $\varepsilon_{ds} > \varepsilon_p$

$$\sigma_d = f_r \cdot f_c \left[1 - \left(\frac{\varepsilon_d - \varepsilon_p}{2\varepsilon_o - \varepsilon_p}\right)^2 \right] \qquad \text{------(2)}$$

where,fr is $1/\lambda$,and λ is expressed by the following equation[10],

$$\lambda=\sqrt{0.7+\varepsilon_1/\varepsilon_d} \qquad \text{------(3)}$$

When the stress-strain relation of concrete between diagonal cracks is transformed into the stress block shown in Fig. 2, k_1 will be according to the following equations:

Case of $\varepsilon_{ds} \leqq \varepsilon_p$

$$k_1=\frac{\varepsilon_{ds}}{\varepsilon_p}\left(1-\frac{\varepsilon_{ds}}{3\varepsilon_p}\right) \qquad \text{------(4)}$$

Case of $\varepsilon_{ds} > \varepsilon_p$

$$k_1=\left(1-\frac{1}{(2\lambda-1)^2}\right)\cdot\left(1-\frac{\varepsilon_p}{3\,\varepsilon_{ds}}\right)+\frac{\varepsilon_{ds}}{(2\lambda-1)^2\cdot\varepsilon_p}\cdot\left(1-\frac{\varepsilon_{ds}}{3\varepsilon_p}\right) \qquad \text{------(5)}$$

The distance (td) from the member surface to the neutral axis shown in Fig. 2 was considered as the path width of shear flow, and the center of the shear flow was considered to pass through the center of the stress block.

b) Tensile Stress-Strain Curve of Concrete

For the tension stiffening of concrete in this study,the tensile stress-strain curve of concrete of Sato and Shirai[8] shown in Fig. 3 was used. In effect, it was expressed by Eq. (6) assuming the stress-strain relationship before cracking to be linear and a third-order curve shown by Eq. (7) assuming that the tension stiffening of concrete after cracking is zero when reaching the limit of bond. It was presumed that tensile stress distribution of concrete is distributed on the width of the shear flow path shown in (c) of Fig. 2.

Case of $\varepsilon_1 \leqq \varepsilon_{cr}$

$$\sigma_r/f_{cr}=\varepsilon_1/\varepsilon_{cr} \qquad \text{------(6)}$$

Case of $\varepsilon_1 > \varepsilon_{cr}$

$$\sigma_r/f_{cr}=1-2.748X+2.654X^2-0.906X^3 \qquad \text{------(7)}$$

where,

$$X=(\varepsilon_1-\varepsilon_{cr})/(\varepsilon_{BU}-\varepsilon_{cr})$$

c) Stress-Strain Curve of Reinforcement

Assuming that longitudinal bars and stirrups to resist stresses only in their respective axial directions, and that the stress-strain relationship of reinforcement is one of a completely elastic body,
the following will result:

$$\sigma_{si}=E_s\cdot\varepsilon_i \qquad \varepsilon_i < \varepsilon_{iy} \qquad \text{------(8)}$$

$$\sigma_{si}=\sigma_{iy} \qquad \varepsilon_i \geqq \varepsilon_{iy} \qquad \text{------(9)}$$

$$\sigma_{sh}=E_s\cdot\varepsilon_h \qquad \varepsilon_h<\varepsilon_{hy} \qquad \text{------(10)}$$

$$\sigma_{sh}=\sigma_{hy} \qquad \varepsilon_h\geqq\varepsilon_{hy} \qquad \text{------(11)}$$

2.2 Analytical Model

When an RC member is subjected to torsion, by applying the assumptions of a) and b) in the preceding section, the principal compression, principal tension, and shear-stress distribution in the direction of member cross-sectional depth will be as shown in Fig. 4 before crack occurrence, and as shown in Fig. 5 after occurrence. That is, when the principal stress distribution in this direction is considered, a biaxial compressive-tensile stress state is formed from the member surface to the cross section center before occurrence of diagonal cracking and in the vicinity of the member surface after occurrence.

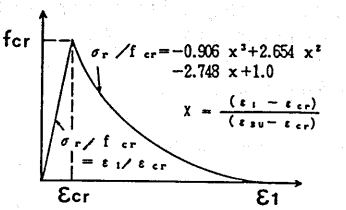

Fig.3 Tensile Stress-Strain Curve of Concrete

This analytical model considers the parts in compression-tension states shown in Figs. 4 and 5 as plate elements in biaxial states, and by using the assumption of c), it will be as shown in Fig. 6.

Vecchio and Collins[12] have expressed this RC member plate element similarly for the case of being subjected to shear.

2.3 Equilibrium Condition Equation

The following equation is obtained for the analytical model shown in Fig. 6 by taking the equilibrium of force in the direction of 1 (longitudinal reinforcing bar).

$$\int_A\sigma_1\,dA=\int_{Ac}\sigma_{c1}\,dA_c+\int_{As}\sigma_{s1}\,dA_s \qquad \text{------(12)}$$

where, the reduction in cross-sectional area of concrete due to reinforcement is small so that when it is ignored Eq. (12) will become Eq. (13).

$$\sigma_1=\sigma_{c1}+\rho_{s1}\cdot\sigma_{s1} \qquad \text{------(13)}$$

Further, as the plate element of an RC member subjected to pure torsion is in a field of pure shear, and Eq. (13) will become Eq. (14).

$$0=\sigma_{c1}+\rho_{s1}\cdot\sigma_{s1} \qquad \text{------(14)}$$

Considering the same for the h(stirrup) direction,

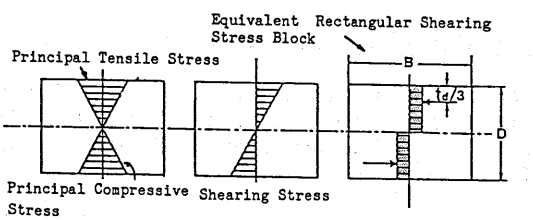

Fig.4 Stress Distribution in the Direction of Cross Sectinal Depth (Before Cracking)

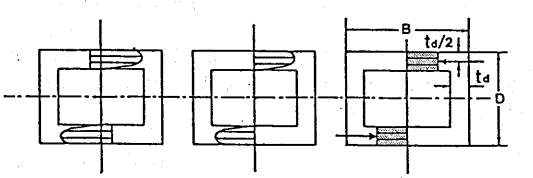

Fig.5 Stress Distribution in the Direction of Cross Sectinal Depth (After Cracking)

Eq. (15) is obtained.

$$0=\sigma_{ch}+\rho_{sh}\cdot\sigma_{sh} \qquad \text{------(15)}$$

Next, by applying Mohr's stress circle shown in Fig. 7 regarding concrete stress, the equilibriums of the 1 and h axes and shear stress will be expressed by the following equations:

$$-\sigma_d\cdot\cos^2\alpha+\sigma_r\cdot\sin^2\alpha+\rho_{sl}\cdot\sigma_{sl}=0 \qquad \text{------(16)}$$

$$-\sigma_d\cdot\sin^2\alpha+\sigma_r\cdot\cos^2\alpha+\rho_{sh}\cdot\sigma_{sh}=0 \qquad \text{------(17)}$$

$$\tau_d=(\sigma_d+\sigma_r)\sin\alpha\cdot\cos\alpha \qquad \text{------(18)}$$

Further, when the second terms on the left sides of Eqs. (16) and (17) are omitted, these equations will be the same as the equations based on the conventional three-dimensional truss model.

Torque can be obtained by the equation of Bredt[4].

$$T=2A_0\cdot t_d\cdot\tau_d \qquad \text{------(19)}$$

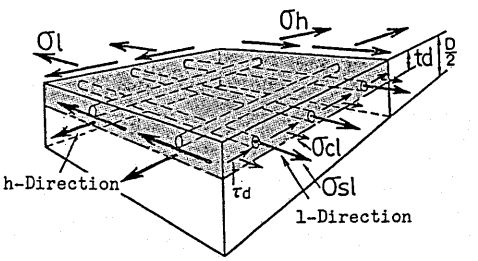

Fig.6 Analytical Model

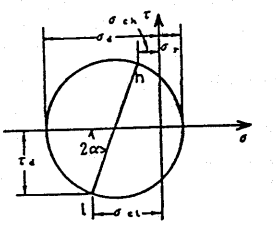

Fig.7 Mohr's Stress Circle

2.4 Kinematic Condition

Mohr's strain circle shown in Fig. 8 can be applied by using the average strain of concrete and reinforcement for the plate element as shown in Fig. 6, and the strains and shear strains in the 1- and h-axis directions will be given as follows:

$$\varepsilon_l=-\varepsilon_d\cdot\cos^2\alpha+\varepsilon_1\cdot\sin^2\alpha \qquad \text{------(20)}$$

$$\varepsilon_h=-\varepsilon_d\cdot\sin^2\alpha+\varepsilon_1\cdot\cos^2\alpha \qquad \text{------(21)}$$

$$\gamma_{lh}=2(\varepsilon_d+\varepsilon_1)\sin\alpha\cdot\cos\alpha \qquad \text{------(22)}$$

Further, from Mohr's strain circle, the crack angle will be according to Eq. (23), the principal tensile strain according to Eq. (24), and the shear strain according to Eq. (25).

$$\tan^2\alpha=(\varepsilon_l+\varepsilon_d)/(\varepsilon_h+\varepsilon_d) \qquad \text{------(23)}$$

$$\varepsilon_1=\varepsilon_d+\varepsilon_l+\varepsilon_h \qquad \text{------(24)}$$

$$\gamma_{lh}=\varepsilon_l\cdot\cot\alpha+\varepsilon_h\cdot\tan\alpha+\varepsilon_d/(\sin\alpha\cdot\cos\alpha) \qquad \text{------(25)}$$

On the other hand, the angles of twist will respectively be expressed by the following equations based on the Compression Field Theory[2] and the thin-shell elastic theory[4].

$$\theta=\varepsilon_{ds}/(2t_d\cdot\sin\alpha\cdot\cos\alpha) \qquad \text{------(26)}$$

$$\theta=\gamma_{th}\cdot P_o/(2A_o) \qquad \text{------(27)}$$

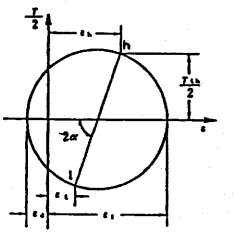

Fig.8 Mohr's Strain Circle

where, by letting Eq. (26) for twist angle computation obtained by the Compression Field Theory and Eq. (27) for twist angle computation obtained by the thin-shell elastic theory, the path width (td) of shear flow will be as follows:

$$t_d=\frac{A_o\cdot\varepsilon_{ds}}{P_o(\varepsilon_l\cdot\cos^2\alpha+\varepsilon_h\cdot\sin^2\alpha+\varepsilon_d)} \qquad \text{------(28)}$$

2.5 Development of Constitutive Equation

Substituting Eq. (23) in Eq. (28), and by respectively eliminating ε_l and ε_h, the following equations will be obtained:

$$\cos^2\alpha=\frac{A_o\cdot\varepsilon_{ds}}{2P_o\cdot t_d(\varepsilon_l+\varepsilon_d)} \qquad \text{------(29)}$$

$$\sin^2\alpha=\frac{A_o\cdot\varepsilon_{ds}}{2P_o\cdot t_d(\varepsilon_h+\varepsilon_d)} \qquad \text{------(30)}$$

From Eqs. (20) and (21), $\sin^2\alpha$ and $\cos^2\alpha$ will be according to the following equations:

$$\sin^2\alpha=\frac{\varepsilon_l+\varepsilon_d\cdot\cos^2\alpha}{\varepsilon_1} \qquad \text{------(31)}$$

$$\cos^2\alpha=\frac{\varepsilon_h+\varepsilon_d\cdot\sin^2\alpha}{\varepsilon_1} \qquad \text{------(32)}$$

Concerning reinforcing bar strain (ε_l) in the 1 direction, by substituting Eqs, (29) and (31) in the equilibrium equation (16), Eq. (33) is obtained. Regarding handling of σ_{sl} in Eq. (33), by substituting Eq. (8) in Eq. (33) before reinforcing bar yielding, and Eq. (9) after yielding, it is possible to obtain ε_l at the respective states.

$$(\varepsilon_l+\varepsilon_d)(\rho_{sl}\cdot\sigma_{sl}+\sigma_r\cdot\varepsilon_l/\varepsilon_1)=\frac{A_o\cdot\varepsilon_{ds}(\sigma_d-\sigma_r\cdot\varepsilon_d/\varepsilon_1)}{(2P_o\cdot t_d)} \qquad \text{------(33)}$$

Similarly, concerning computation of reinforcing bar strain (ε_h) in the h direction, Eq. (34) is obtained by substituting Eqs. (30) and (32) in the equilibrium equation (17). The ε_h at the respective states can be obtained by substituting Eq. (10) for σ_{sh} in Eq. (34) before reinforcing bar yielding and Eq. (11) after yielding

$$(\varepsilon_h+\varepsilon_d)(\rho_{sh}\cdot\sigma_{sh}+\sigma_r\cdot\varepsilon_h/\varepsilon_1)=\frac{A_o\cdot\varepsilon_{ds}(\sigma_d-\sigma_r\cdot\varepsilon_d/\varepsilon_1)}{(2P_o\cdot t_d)} \qquad \text{------(34)}$$

2.6 Analytical Procedure

The flow chart of analysis will be as follows:
1) Give the cross-sectional configuration, reinforcement arrangement, and the physical properties of reinforcing bars and concrete.
2) Select the value of strain (ε_{ds}) of concrete.
3) Assume the depth (td) of shear flow.
4) Assume the principal strain(ε_1).
5) Calculate k_1 from Eqs. (4) and (5), λ from Eq. (3), and σ_d from Eq.(1) or Eq. (2).
6) Calculate ε_l from Eq. (33) and ε_h from Eq. (34).
7) Calculate principal tensile strain ε_1 from Eq. (24).
8) Repeat 4) to 8) until the error in ε_1 becomes less than the allowable value.
9) Calculate crack angle from Eq. (23) and shear flow depth from Eq. (28).
10) Repeat 3) to 10) until the error in t_d becomes less than the allowable value.
11) Calculate torque (T) using Eq. (19) and angle of twist (θ) using Eq. (26).
12) Return to 2) and repeat the procedure varying the value of concrete strain (ε_{ds}).

3.OUTLINE OF EXPERIMENTS

3.1 Experimentation Program and Specifications of Specimens

With the objective of finding the behavior of torsional resistance of RC members subject to pure torsion, loading experiments were carried out making square cross-sectioned specimens with reinforcement quantity constant and varying cover (distance from member surface to stirrup center) in 3 ways (hereafter referred to as Series C, and square cross-sectioned specimens of height 300mm,width 300mm, and length 2,500mm with reinforcement ratio varied in 3 ways (hereafter referred to as Series S. The experimentation program regarding these specimens is given in Table 1.

An example of the cross-sectional dimensions and reinforcement arrangements of specimens on which loading tests were carried out is shown in Fig. 9.

Table 1 Experimentation Program

Name	No.	Width (cm)	Height (cm)	Thickness of Cover Concrete(cm)	A_{sl} (cm^2)	Stirrup	
						A_{sh} (cm^2)	s(cm)
Series C	C1	20	20	0.5	5.41	0.676	12
	C2	25	25	3.0	5.41	0.676	12
	C3	30	30	5.5	5.41	0.676	12
Series S	S1	30	30	2.0	5.41	0.676	12
	S2	30	30	2.0	8.11	0.676	8
	S3	30	30	2.0	10.8	0.676	8

Table 2 Physical Properties of Reinforcing Bars

	Area (cm^2)	Yield Strength (N/mm^2)	Tensile Strength (N/mm^2)	Modulus of Elasticity (N/mm^2)
D10	0.676	398	578	0.19×10^6

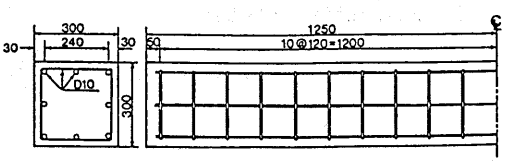

Fig.9 Cross-Sectinal Dimensions and Reinforcement Arrangements of Specimen

3.2 Materials

The reinforcing bars used were SD-30, D-10, and the results of tension tests are given in Table 2.

The concrete used had a target compressive strength of 300kgf/cm^2(28.4 kN/mm^2), and the results of tests are given in Table 3.

3.3 Loading Method

Loading tests were made using a strain-control type apparatus, and a brief sketch of the loading method is shown in Fig. 10.

4. COMPARISON STUDY OF EXPERIMENTAL AND ANALYTICAL RESULTS

4.1 Influence of Tension Stiffening of Concrete on Torsional Behavior of RC Member

There have been many studies made concerning tension stiffening of concrete before and after crack occurrence with members subjected to bending moment and shear force as objects, and to summarize them, there are two ways of thinking, the thinking of the CEB-FIP Code[8] which maintains that there is influence on coefficient of elasticity of reinforcing bars which are tension materials, and the thinking that with concrete under tensile stress, the tensile stress increases linearly with increase in tensile strain before crack occurrence and gradually decreases with increase in tensile strain after crack occurrence[9]. However, to use the conventional three-dimensional truss and diagonal flexure models with the purpose of continuously grasping the conditions before and after crack occurrence introducing the influences of these, since these models assume in the first place states in which diagonal cracks have completely developed, it may be said that there is a discrepancy in the basic assumption. When torsional loading experiments are made, the load-deformation curve before crack occurrence of an RC member subjected to torsion is practically uninfluenced by the reinforcement quantity and is governed by the tensile stress of the concrete, while in concrete struts after crack occurrence, tensile stress perpendicular to the cracks is produced with bond between reinforcing bars and concrete as the medium, and from the fact that the tension stiffening of concrete is the governing allocation of strength of an RC member subjected to torsion, the study of this analysis giving consideration to this influence will be as described below.

Table 3 Physical Properties of Concrete

Series	Compressive Strength (N/mm^2)	Tensile Strength (N/mm^2)	Modulus of Elasticity (N/mm^2)
C	34.8	2.9	0.22×10^5
S	29.4	2.7	0.20×10^5

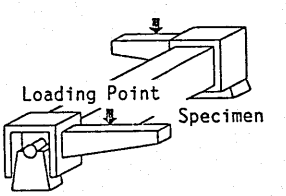

Fig.10 Loading Method

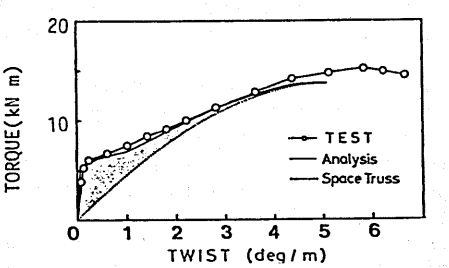

Fig.11 Relationship between Acting Torque and Twist per Unit Length (Specimen C1)

The relationship between acting torque (T) of Specimen C with concrete cover of 0.5 cm which is close roughly to zero and twist (θ) per unit length will be as shown in Fig. 11, and can be divided into the following 4 zones[7] having features normally attributed to them from T-θ curves.

That is, the first zone is the state before the initial diagonal crack is formed in the member, where the T- curve becomes more or less identical to the relationship obtained by elastic theory assuming the concrete to be a monolith.

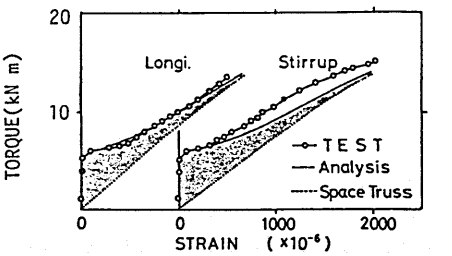

Fig.12

Relationship between Torque and Reinforcing Bar Strain

The second zone is the zone in which torsional stiffness is lowered greatly with initial crack occurrence compared with Zone 1, and the number of cracks is increased.

The third zone is a zone in which the number of cracks is not increased and only crack widths are increased. Reinforcing bars yield near the end of this zone.

Lastly, in the fourth zone, stiffness again declines, ultimate strength is reached, and secondary cracks are formed.

In the conventional analyses based on truss models, as shown by the dotted line in Fig. 11, only the trend of experimental values in the vicinity of maximum strength, or, from Zone 3 to Zone 4, was grasped. The reason for this is that with a three-dimensional cracks have completely developed, and the constitutive equation has been obtained from the equilibrium condition and the adaptation condition of strain ignoring tension stiffening of concrete. As shown by the solid line in Fig. 11, this analysis which considers the tension stiffening of concrete is capable of accurately grasping the trends of experimental values before and after crack occurrence and at the ultimate state.

The tension stiffening of concrete also affects the relationship between torque and reinforcing bar strain, and as shown in Fig. 12, it was succeeded in analytical values estimating with good accuracy the average strain(average value from 8 strain gauges each attached to axial-direction reinforcing bars and stirrups at 2 cm intervals) of experimental values for all zones.

As described above, since the influence of tension stiffening of concrete indicated by the second terms at the left sides of Eqs. (16) and (17) could not be taken into consideration with the conventional three-dimensional truss model, the allocation of reinforcing bar resistance to the same torque became larger than actual to result in overestimation. However, in the present analysis, the tension stiffening of concrete at and after crack occurrence was considered as shown in Fig. 3, so that allocation of reinforcing bar resistance became smaller than for that based on the three-dimensional truss model, and it was possible to grasp the trends of the individual zones in the experimental values. If the strength borne by reinforcement before occurrence of cracking in an RC member subjected to pure torsion is ignored because it is small, the compressive stress σ_d of concrete and tensile stress σ_r of concrete in the equilibrium equations (16) and (17) become equal, and are identical to the equatons when subjected to pure shear. However, Eqs. (16) and (17) indicate that after occurrence of cracking, tensile stress σ_r of concrete is decreased as shown in Fig. 3, and

when σ_r is zero it will be the same as with the three-dimensional truss model, and this may be said to be an analysis which rationally grasps actual torsional behavior.

4.2 Influence of Cover Concrete of RC Member on Torsional Behavior

In calculation of ultimate torque using the three-dimensional truss model, the manner in which the shear flow path location is set out has an extremely great influence on strength, so that there have been numberous concepts offered since Rausch's formula up to the present. Furthermore, factors causing deterioration such as carbonation and salt damage have become prominent so that there is a trend for concrete cover to be made thick, and the influence of concrete cover on this type of member has become a matter that cannot be ignored. However, there are still many points about handling of cover concrete both in analyses and experiments that are not clear, and especially, in case of estimating the deformation behavior at any loading stage, it is not an exaggeration to say that unless the changes in the shear flow path locations from before occurrence of cracking until the ultimate state are accurately grasped tied in with cover concrete, the torsional resistance mechanism of this type of member cannot be discussed. Therefore, in this section, studies will be made, experimentally and analytically, of the influences of concrete cover on the torsional behaviors of RC members,

a) Load-Deformation Curve

Spalling of cover concrete of RC members subjected to torsion has been pointed out by Collins and Mitchell[3], while Hsu and Mo[4] maintained that only when the ratio of the distance from member surface to inner side of stirrup to width of path of shear flow is higher than 0.75 should spalling phenomena be applied, and in case of a ratio lower than 0.75, strength calculations are made including cover concrete. Later, in the study by Ewida and McMullen[11], it was considered that this spalling occurred after maximum strength has been reached.

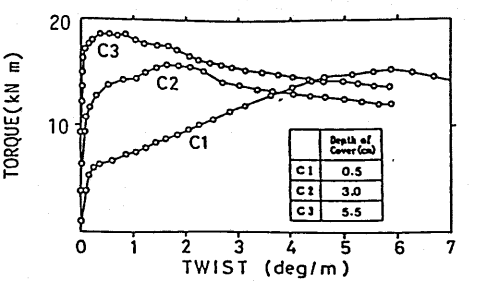

Fig.13 Relationship between Acting Torque and Twist (Series C)

The results of experiments on the relationship between acting torque (T) and twist (θ) in Series C where thickness of cover was varied are shown in Fig. 13. Series C is the one where quantity of reinforcing steel was constant and thickness of cover was varied at 0.5, 3.0, and 5.5 cm.

The strength at which diagonal cracks occurred showed a tendency to increase since the cross section would become larger with increased thickness of cover.

The strength after occurrence of cracking showed prominant decrease due to spalling the greater the thickness of cover, this spalling phenomenon being strongly affected by cover thickness, with maximum strength reached immediately after crack occurrence in case of C3 of large thickness of cover, the strength gradually declining along with advancement of deformation to approach in the end the load-deformation curve of Spcimen C1 of cover roughly close to 0 cm. That is, with Specimen C1, deformation progressed along with strength after occurrence of cracking with maximum strength of 1.36 tf m(13.3 kN/mm^2) reached at twist of 5.82 deg/m, while with Specimen C2 of cover 3.0 cm, the maximum

strength was 1.46 tf m(14.3 kN/mm^2) when twist was 1.7 deg/m. Further, with Specimen C3 of cover 5.5 cm, maximum strength of 1.76 tf m(17.2 kN/mm^2) was reached when twist immediately after crack occurrence was 0.65 deg/m, and it was recognized that twist at maximum strength decreased with increased cover. Therefore, it was shown by this figure that spalling occurred at a comparatively early period as cover became thicker.

Next, the experimental and analytical values of the relationships of acting torque (T) and twist (θ) per unit length of Series C and S are shown in Figs. 14 and 15, respectively.

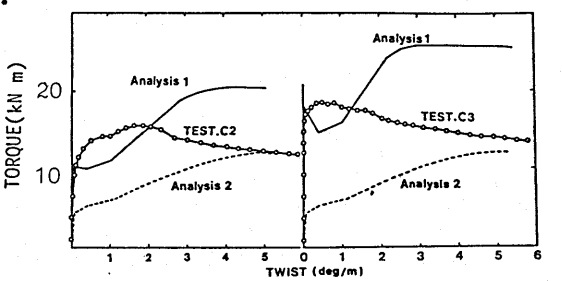

Fig.14 Experimental and Analytical Values of the Relationships between Torque and Twist (Series C)

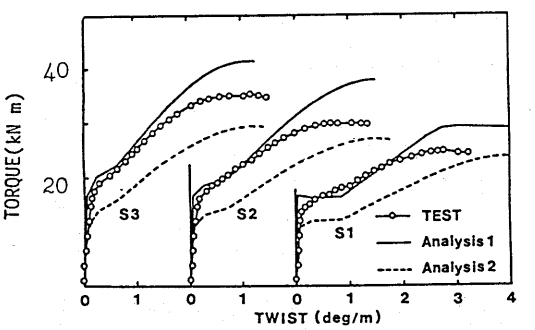

Fig.15 Experimental and Analytical Values of the Relationships between Torque and Twist (Series S)

In performing analyses, the allocations of tensile forces borne by concrete were taken into account, and studies were made of the two cases of Analysis 1 with path width of shear flow taken from the surface considering that concrete would not be spalled, and Analysis 2 considering cover concrete to be spalling and taking the path width from the center line of stirrups.

Based on the spalling of cover concrete shown in Fig. 12, it was possible in Analysis 1 for the trend of experimental values in the vicinity of the time of diagonal crack occurrence to be evaluated, and in Analysis 2, the trend in the vicinity of ultimate strength with regard to Specimens C2 and C3 for which maximum strengths had been determined.

On the other hand, with regard to Series S shown in Fig. 15, in which maximum strength was not determined by spalling of cover concrete, it was possible in Analysis 1 to evaluate the behaviors at and after occurrence of diagonal cracking, where in the vicinity of maximum strength the experimental values were exceeded but the vicinity of maximum strength was excluded. However, in Analysis 2, although strengths at and after cracking were exaluated on the low side, there was good agreement with experimental values.

According to the foregoing, spalling starts more at an initial stage of deformation the smaller that the cross section is even with identical thicknesses of cover, that is, the larger the ratio of cover thickness to cross section side length, while subsequently, it proceeds gradually, until in the end the concrete cover is completely spalled.

As shown in Fig. 14 and 15, the difference between Analyses 1 and 2 lies in from where the width of the shear flow path is taken, and it can be comprehended that influence of the manner of handling shear flow on the relationship between torque and deformation is extremely great. Consequently, it is thought that in calculation of maximum torque and deformation at that time, the method of taking

the width of the shear flow path from the center line of stirrups considering spalling of concrete will be on the conservative side in design, and gives reasonable values in step with the results of experiments.

In any event, when estimating strength-deformation from the time of crack occurrence until maximum strength, it is thought to be necessary for the spalling phenomenon due to the influences in the thickness of cover and cross-sectional dimensions to be quatitatively exaluated.

b) Cracking Propersies

Spalling of the concrete cover can be comprehended also from the cracking pattern shown in Fig. 16. With Specimen C3 of thick cover, spalling occurs with small deformation, that is, θ =0.65 deg/m, and stress transmission no longer takes place between cover concrete, axial reinforcement, and stirrups, as a result of which the number of cracks at cover concrete is not increased after spalling and crack intervals are large compared with Specimen C1. Specimen C1 has cover of 0.5 cm with the concrete surface and stirrup surface on the same plane and spalling does not occur. Crack dispersion becomes better than for the cover portion of Specimen C3, with the number of diagonal cracks increased. Furthermore, with Specimen C3 also, cracking properties similar to those of Specimen C1 are seen at the part inside stirrups removing cover concrete, and the cracking properties clearly differ between the cover portion and the portion surrounded by stirrups.

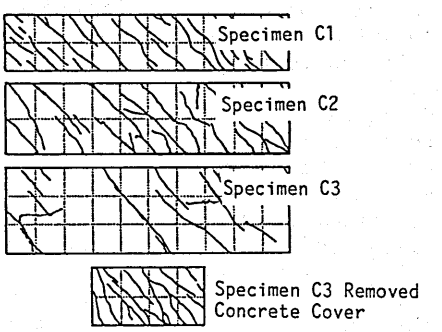

Fig.16 Cracking Pattern (Series C)

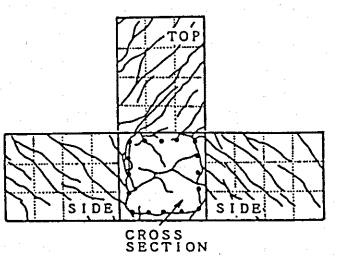

Fig.17 Cracking Pattern (Series S)

After completion of loading tests, specimens were cut perpendicularly to the longitudinal direction, and the condition of development of cracks at a transverse cross section is shown in Fig. 17. As this figure shows, the initial crack first occurs at the surface of the member at an angle of 45 deg from the axial direction later growing inward, and extending to approximately 80 percent of the member width at the time of failure. The compression depth in the theory using a diagonal flexure model is taken from the surface of the member, but as shown in the cracking pattern diagram, cracks are formed along the reinforcing bar cage also showing that cover concrete had spalled. In effect, since cover concrete and reinforcement were not integral, it was ascertained from this diagram that it is reasonable to compute maximum strength removing the spalled portion. Consequently, for the path of shear flow in the three-dimensional truss model also, it is a more rational and reasonable method to exclude the spalled portion with regard to maximum strength.

c) Strain Distribution and Compression Depth of Concretein Direction of Depth of Member Cross Section

Concrete gauges were attached to member surfaces at 45-deg angles from the member axes, and embedment gauges were arranged at locations from the surfaces determined beforehand. The strain distributions from these are shown specimen by specimen in Figs. 18 and 19.

According to these figures, the locations of neutral axes coincided with the centers of the square cross sections before occurrence of diagonal cracks, but after occurrence, the neutral axes shifted abruptly to near the concrete surfaces, after which, along with increases in deformation, the distances from the concrete surfaces increased slightly. That is, with Specimen C1 of cover close to 0 cm, the depth to the neutral axis after occurrence of cracking changed from 2.5 cm to 3.8 cm at maximum strength. In analysis using Eq. (28), the depth was 2.4 cm immediately after crack occurrence and 3.9 cm at maximum strength for good agreement with the experimental values. On the other hand, with Specimen C2 of cover thickness 3.0 cm, the depth of the neutral axis was 3.2 cm after occurrence of cracking, later becoming 6.8 cm at the end as deformation increased, but in analysis, the depth of the neutral axis after crack occurrence was 3.0 cm, and 4.0 cm at the end, the final depth of the neutral axis being much smaller than the experimental value. In this regard, when it was considered that cover concrete would be spalled off in the end, and the thickness of concrete cover of 3.0 cm was deducted, the result was 3.8 cm to agree roughly with the analytical value.

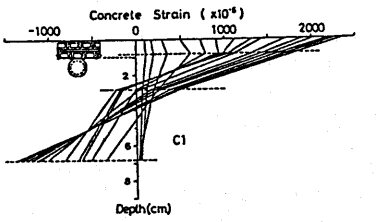

Fig.18 Strain Distribution of Concrete in Direction of Depth of Cross Section (Specimen C1)

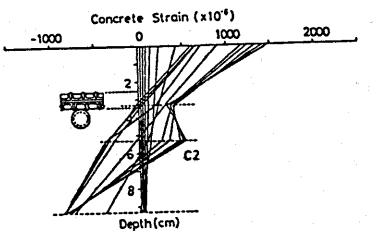

Fig.19 Strain Distribution of Concrete in Direction of Depth of Cross Section (Specimen C2)

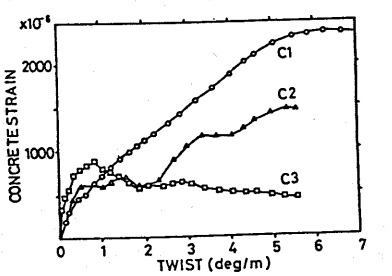

Fig.20 Surface Strain Distribution of Specimen C1, C2 and C3

The surface strain distributions of Specimens C1, C2,and C3 are shown in Fig. 20 to explain such spalling phenomena. Firstly, in the case of Specimen C1, concrete strain is increased as deformation advances since spalling has not occurred, but the concrete strain of C3 increases linearly until crack occurrence, after which on reaching maximum strain of 900 at twist of 1.02 deg/m it begins to decline, and in the end it becomes 450 .

As a consequence, the influences of cover concrete and the path width of shear

flow on the torsional behavior are conjectured to be as described below. That is, the compression depth existing on the surface side of the member after cracking provides monolithic resistance through the medium of bond between reinforcement and concrete, but spalling begins at an earlier stage the greater the thickness of concrete cover for gradual loss of the integrity, and as a result the compression depth increases to be in equilibrium with tensile force. Subsequently, the compression depth extends to the interior enclosed by reinforcement and in the end the cover spalls.

4.3 Torsional Resistance of RC Member

Early studies on torsion[3] and the current ACI Building Code Requirements[13] use Eq. (35) for calculating maximum strength.

In effect, maximum strength (T_u) is considered as the sum of crack resistance (T_c) and resistance (T_s) by reinforcement of a three-dimensional truss structure. The Standard Specifications of the Japan Society of Civil Engineers[4] maintain that such a concept is unreasonable since torsional resistance from crack resistance cannot be expected at maximum strength, and considers only resistance (T_s) by the reinforcement in the truss structure after occurrence of cracking.

However, with the analytical method described here, the load-deformation relationship can be grasped continuously from before occurrence of cracking until ultimate strength through calculation with only T_c at cracking and then introducing tension stiffening between concrete struts after crack occurrence so that it can be expressed how T_c is predominant at the initial stage after crack occurrence,but gradually, it declines as deformation increases, and finally, T_s becomes predominant. Therefore, by using this analytical method, it becomes possible to grasp the torsional behaviors of RC members at the limit state with good accuracy in regard to torsional crack width and displacement-deformation.

5. CONCLUSIONS

This study was made with the objective of learning about the torsional behavior of reinforced concrete members, and within the scope of this study, it was possible to draw the following conclusions:

(1) With the conventional three-dimensional truss model, deformations at Zones 1,2, and 3 are overestimated, but with the present analytical method which takes into consideration tension stiffening of concrete,the torsional resistance behavior of a reinforced concrete member can be estimated with good accuracy from before occurrence of cracking up to the time of failure.

(2) The depth of compression axis or the width of the shear flow path (t_d) can be estimated by Eq. (28) which is obtained by assuming that the twist determined by the Compression Field Theory and the twist based on the thin-shell elastic theory are equal, and as a result there is good agreement with experimental results.

(3) The phenomenon of spalling of the cover of a reinforced concrete member subjected to torsion is not something which occurs after reaching maximum strength, but begins from an early stage before maximum strength, with spalling occurring at an earlier stage of loading the greater the reinforcement strain and the larger the thickness of cover.

(4) The computation method considering the full cross section as effective in calculating crack resistance and taking into account a softening phenomenon of concrete for the cross section considering cover to have spalled is an analytical method which aptly grasps the actual torsional phenomenon of a reinforced concrete member,and may be said to be reasonable.

(5) The location of the neutral axis coincides with the center of the rectangular cross section before occurrence of cracking, but shifts abruptly to near the surface of the member after cracking so that the thin-shell theory can be applied even for a member with a solid cross section.
(6) At any stage of loading the resistance provided by concrete is predominant in the load resistance mechanism before crack occurrence, but as deformation progresses after crack occurrence, the resistance provided by concrete declines, with the resistance by the truss structure becoming predominant in the end.
(7) Hereafter, in theoretical studies of load-deformation in any state, there will be a necessity to study stress decline due to spalling and variation in compression depth of concrete struts.

NOTATION

A_o = Area enclosed by the center line of shear flow
A_{sl} = Total area of longitudinal steel
A_{sh} = Cross sectional area of one leg of a transverse steel bar
f_c = Cylinder compression strength of concrete
f_r = Coefficient for softening effect
k_1 = Average stress divided by peak stress in the stress block
P_h = Perimeter of the center line of a transverse hoop bar
P_o = Perimeter of the center line of shear flow
T = Torsional moment
s = Spacing of transverse hoop bar
t_d = Effective depth of the compression zone in the diagonal concrete struts
α = Angle of inclination of the diagonal compression struts
γ_{th} = Shear distorsion at the center line of shear flow
ε_1 = Principal tensile strain in concrete
ε_{BU} = Bond limit strain between steel and concrete
ε_{cr} = Tensile strain in concrete
ε_d = Concrete strain of shear flow in the diagonal concrete struts
ε_{ds} = Strain at the surface of the diagonal concrete struts
ε_h = Strain in stirrup
ε_l = Strain in longitudinal reinforcing bar
ε_o = Strain at maximum stress of non-softened concrete, taken as 0.002
θ = Angle of twist per unit length
ρ_{sl} = $A_{sl}/(P_o \cdot t_d)$
ρ_{sh} = $A_{sh} \cdot P_h/(P_o \cdot t_d \cdot s)$
σ_{ch} = Stress in concrete in the direction of transverse reinforcing bar
σ_{cl} = Stress in concrete in the direction of longitudinal reinforcing bar
σ_d = Average compressive stress in the longitudinal concrete struts
σ_r = Tensile stress in concrete
σ_{hy} = Yield strength of longitudinal reinforcing bar
σ_{ly} = Yield strength of stirrup
σ_{sh} = Stress in stirrup
σ_{sl} = Stress in longitudinal reinforcing bar
τ_d = Shearing stress at the center line of shear flow

REFERENCES

1) Rausch,E.:Design of Reinforced Concrete in Torsion, Techische Hochschule Berlin, pp.53,1929
2) Lessig,N.N.:Determination of Load-Carrying Capacity of Rectangular Concrete Elements Subjected to Flexure and Torsion, Trudy No.5, Institut Betonai Zhelezabetona (Concrete and Reinforced Concrete Institute), Moscow, pp.5-28 (in

Russian), Translated by Portland Cement Association, Foreign Literature Study, No.371
3) Collins,M.P. and Mitchell, D.:Shear and Torsion Design of Prestressed Concrete Beams, PCI Journal, Vol.25, No.5, pp.32-100, Sep.-Oct.,1980
4) Hsu,T.T.C. and Mo, Y.L.:Softening of Concrete in Torsional Members, Univ. of Houston, Civil Eng. Dept., Research Report, pp.1-107, March 1983
5) Rangan,B.V., Staley, R.F. and Hall, A.S. :Behavior of Concrete Beams in Torsion and Bending, Journal of the Structural Division, ASCE, Vol.103, ST-4,pp.749-772, Apr.1978
6) Ewida,A.A. and McMullen,A.E. :Torsion-Shear-Flexure interaction in reinforced concrete members, Magazine of Concrete Research, Vol.33, No.115, pp.113-122, June 1981
7) Nagataki,S., Okamoto,T., Lee,S.H. and Yamaoka,S. :A Study of Torsional Properties of Reinforced Concrete Members(in Japanese), Proceeding of the Japan Society of Civil Engineers, No.372/V-5, pp.157-166,1986
8) Reported by ACI Committee 224:Cracking of Concrete Members in Direct Tension, ACI Journal, Vol.83, No.1, pp.3-13, Jan.-Feb.,1986
9) Sato,M. and Shirai,N. :A Study on Elastic-Plastic Properties of Earthquake-Proof Wall Builded by Reinforced Concrete (in Japanese), Annual Convention Report of Architectual Institute of Japan, pp.1615-1618, 1978
10) Vecchio,F. and Collins,M.P. :Stress-Strain Characteristics of Reinforced Concrete in Pure Shear, IABSE Collequuim Advanced Mechanics, No.115, pp.113-122, June 1981
11) McMullen,A.E. and El-Degwy,W.M.:Prestressed Concrete Tests Compared With Torsion Theories, PCI Journal, Vol.30, No.5, pp.96-127, Sep.-Oct.,1985
12) Vecchio,F. and Collins,M.P.:The Modified Compression Field Theory for Reinforced Concrete Elements Subjected to Shear, ACI Journal, Vol.83, No.1, pp.219-231, Mar.-Apr. 1986
13) ACI 318-77 :Building Code Requirment for Reinforced Concrete Institute, Detroit,1977
14) Japan Society of Civil Engineers :Standard Specification For Design and Construction of Concrete Structures, Part 1 (Design),1986